

Defect Identification and Repair Algorithm for Polymer Light Emitting Diodes

Liang-Jiun Chen, Chih-Jian Lin, Jyh-Chyang Chen, Jane Chang and Kevin Cheng
OES/Industrial Technology Research Institute, Hsinchu, Taiwan, Republic of China
E-mail: chenlj@itri.org.tw

Abstract. *The innate character of ink jet instability sometimes causes device defects in polymer light emitting diodes (PLED). This study develops an image-processing method to identify defects by methods such as filtering, color processing, background subtraction, dilation, etc. Based upon the defect information and the pre-built ink jet print head library, the amount of ink volume and the location to print on can be appropriately estimated to patch defects. In addition, an optimal printing route can be determined with a specially designed head driving waveform, consisting of pre-oscillations during motion intermission. By this methodology, a 60 pL sized drop from ink jet nozzles can approximately patch the PLED panel with pixel resolution of $240 \times 73 \mu\text{m}$, the QCIF standard. The results demonstrated good accuracy in landing while patching unfilled pixels. However, there are some satellite drop occurrences observed due to the sensitivity of image data threshold level setting. Overall, the confidence level of successful defect identification is larger than 95%. In this paper, an optimal repair route and a strategy about thin film morphology control were also discussed. These approaches are helpful to repair defects and, consequently, increase the yield rate for PLED or other applications by ink jet technology. © 2006 Society for Imaging Science and Technology.*

[DOI: 10.2352/J.ImagingSci.Technol.(2006)50:3(257)]

INTRODUCTION

The technology of Polymer light emitting diodes (PLED) offers many attractive properties for use in display applications. The discovery of electroluminescence in organic molecules and semiconducting polymers has generated considerable interest in display applications based on these materials.^{1,2} In past years, many groups have focused on the challenge to overcome the technical hurdles to realize high-resolution passive displays of PLED.^{3–5} However, some critical technical issues are still left to be resolved, for example, the coffee ring behavior, the ink jet stability control,^{6,7} the bank pattern design,⁸ and the crosstalk issues.⁹ The mask-patterning method has been developed using low molecular weight type organic EL for multicolor displays in past years. For single color of PLED, a spin process is workable. But, for a full color PLED, the spin method turns out to be not viable due to problems in spinning on additional color without affecting the color already in place. Therefore, given the good match between the polymer solution and the ink jet capability, an ink jet patterning method has been developed for multi-color PLED displays.^{10,11}

However, there are some challenges when applying the

ink jet printing process. The film uniformity problem arose in the ink jet printing method, especially around the drop-perimeter. The ring-type behavior causes the film to have different film thickness within pixels. The thick periphery will lead to low efficiency of PLED and the thin center will break down with current leakage. How to ensure uniform film thickness is the key issue to be solved in ink jet printing process. In addition, proper surface treatment of the substrate is critical. If the surface is not well treated, the hydrophilic or hydrophobic interface of the surface will cause the ink droplet to spread or roll forming defects on the surface. Ink jet instability is another key factor for the defect forming, in particular when the print head has large drop deviation or poor nozzle-to-nozzle stability. These intangible behaviors deteriorate the yield rate in fabrication of PLED and cause short lifetime of the panel.

Therefore, this study designs a defect identification algorithm and a patching process on a self-developed ink jet platform. By image identification scheme, versatile defects are recognized. Once these defects are established, the information is analyzed and converted into ink volume necessary for patching by an algorithm similar to the well-known halftoning technique. To maintain the patching process stability, we also design a low driving energy waveform to prevent ink from clogging at nozzles.

DEFECT OBSERVATION

The ink jet method applied to PLED is performed by printing PEDOT on the ITO substrate and then printing PF on the PEDOT layer. Many factors can affect a defect occurrence on PLED panel. Typical examples are: (1) Ink jet instability, in which inappropriate driving waveform creates undesirable satellite drops. (2) Nonuniform surface property on substrate, which causes different wetting effects on pixels. The hydrophilic or hydrophobic properties of the surface difference lead to varied film morphology. Some typical problems came from the uniformity of the plasma surface treatment, substrate cleaning, roughness of the substrate, as well as the dimensional variation of the photo bank. (3) Nozzle clogging, which often occurs as jetting, especially, polymer blended highly volatile solvent. The continuous jetting behavior usually becomes unstable after the nozzle has clogged. It is believed that the high evaporation rate of the ink tends to cause a crusting effect around the orifice, as the local concentration of the ink rapidly increases with time.

This will result in blockage at the openings of the nozzles. From our experience in ink jet printing PLED, three to five minutes of nonprinting period will cause the start-up instability. In the worst case, the ink jet head cannot even discharge. Appropriate driving modulation to free the ink chamber from clogging is needed. (4) Nonuniform layering of PEDOT by ink jet printing, also causing puddling defect in the subsequent PF layer (5) Surface property of the bank changes over a long period of printing time. Typically, the plasma treatment can keep the surface hydrophilic properties about 3 to 4 h. Beyond the period, the bank starts to repel the PF ink and form defects. (6) Environment control problem: Moisture is the major reason for environmental defects. It will change the bank and PEDOT surface characteristics, and deteriorate the device. Detailed defect observation and discussion can be referred to Lin et al.¹²

In this paper, the disclosed patching process is mainly for under-filled pixels. The method includes steps of identifying all defects of the device by image analysis and then obtaining an optimal ink jet printing path of the ink jet head. The ink jet head repairs all defects of the device at the shortest distance along the optimal patching path. The detection and patching are automated to improve the quality and yield of the element.

SURFACE INTERFACE BEHAVIOR

The deposition of ink on a substrate brings new interfaces among dissimilar materials and involves considerations of wettability, spreading effect, interface evolution, and adhesion. The wettability of a substrate by ink is characterized in terms of the contact angle that the ink makes on the substrate. The contact angle, q , is obtained from a balance of interfacial tensions and is defined from Young's equation, according to $slv \cdot \cos q + sls = ssv$, where slv , sls , and ssv are the interfacial tensions at the boundaries between ink (l), substrate (s), and vapor (v). Here, s represents the force needed to stretch an interface by a unit distance. The condition $q < 90^\circ$ indicates that the substrate becomes wet from the ink, and $q > 90^\circ$ indicates nonwetting, with the limits $q = 0$ and $q = 180^\circ$ defining complete wetting and complete nonwetting, respectively.¹³

The contact angle indicates the wettability of ink on the surface of a substrate. For application like PLED by ink jet printing, a drop of polymer ink will come in contact with two different interfaces. Typically, for ink jet printed PEDOT, the PEDOT ink will contact ITO film with hydrophilic interface while contacting the photo bank with the hydrophobic interface. Similarly, for ink jet printed PF, it contacts with PEDOT film with the hydrophilic interface, while contacting the photo bank with the hydrophobic interface. However, the surface interface will dramatically change over time because some treatment method such as the plasma lasts only for a short time duration, for example, three to four hours. When the complete full color ink jet printing and related processes take more than the time limit, it is possible that the number of pixel defects will increase.

INK JET INSTABILITY

The innate character of ink jet instability causes the device defect in the fabrication process, mainly due to the mechanical inertia force faced by acceleration, the initial instability of head driving, and behavior difference across individual nozzle. The mechanical inertia force causes an exponential decay with the printing distance, and it manifested as a landing position variation. Another occurrence of instability is at the beginning of printing. The instability of head driving is caused by unstable ink refilling, and it results in drop size variation. The biggest challenge in printing stability is the control of nozzle-to-nozzle variation. Due to the difference in ink channel length for each nozzle, it is found that the drop size and its break-off behavior varied, even when the driving energy for each nozzle remained the same. Please refer to Song et al. for more details and solution strategies.¹⁴

IMAGE IDENTIFICATION FOR DEFECTS

An image identification methodology for defect recognition followed the study by Lin et al.¹² The procedure included: Capturing image by setting hardware and its optical characteristic, image, processing of captured image, and recognizing the defects in the image through image comparison. The optical hardware setting for the image analysis system includes fine-tuning of CCD color saturation, light source intensity and compensation, magnification and optical focus tuning, etc. The image then requires a pre-processing to establish an image template at the same hardware setting used for calibrating image distortion and enhancing color intensity. For polymer solutions like PEDOT and PF, they are highly transmittant and hard to be observed in thin film thickness. To establish an image template as background before image processing algorithm for these solutions is critical. After that, a pixel to physical coordinate conversion is performed for calculating the real size of image pixel.

For saving calculation time and improving the recognition rate, the image was segmented through a threshold filtering. Then, the image was rotated and aligned to correct the image distortion in CCD capture. The corrected image is then compared with a standard image template, generally, by subtracting the background image, and enhancing the signal to noise ratio. After that, some more pre-processing including noise removal, color range conversion, contrast enhancement, binary transformation, and color plane extraction were used to further enhance the image.

After the image is captured and enhanced, additional techniques such as threshold processing, image operation, morphology, and filtering operation are applied for defect image identification. Several defect types using these image processing techniques will be discussed as follows.

Defect type A: Satellite Drop Occurrence

Here, we utilize a preprocessed image as a template image, which is called a "mask." The result from some of the steps are shown in Figs. 1(a)–1(j). The steps included:

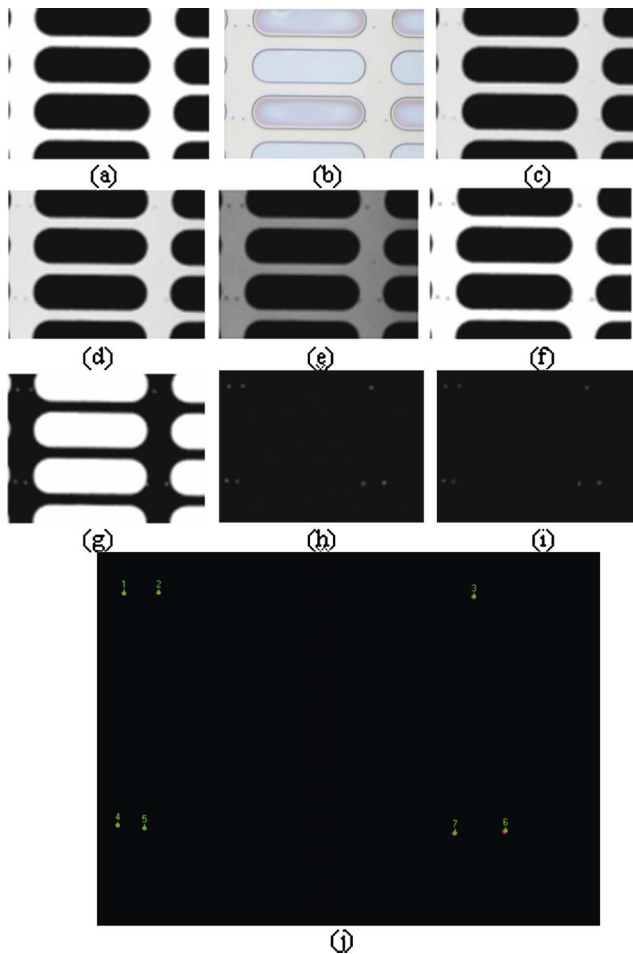


Figure 1. (a)–(j) Identification of satellite drop of PLED image. (a) Template image before ink jet printing of PEDOT. (b) Original image after ink jet printing of PEDOT. (c) Operation AND between template and original image. (d) Color abstraction (e) Image enhancement. (f) Binary operation. (g) Invert image value. (h) Operation AND between template and (g). (i) Filtering. (j) Particle analysis, calculation of particle size, and location.

- (1) Get the ellipse area mask from the file, as shown in Fig. 1(a);
- (2) place the mask into first image buffer;
- (3) get the image of PLED substrate from the file, as shown in Fig. 1(b);
- (4) process the mask and the image of PLED substrate by using operator AND to get the image of the background, as shown in Fig. 1(c);
- (5) extract color plane by using HSL-luminance to transform the image into a grayscale image, as shown in Fig. 1(d);
- (6) image enhancement using exponential function from a look-up table, as shown in Fig. 1(e);
- (7) get the binary image by a pre-determined threshold, as shown in Fig. 1(f);
- (8) invert the binary image, as shown in Fig. 1(g);
- (9) process the image and the mask with operator AND, as shown in Fig. 1(h);

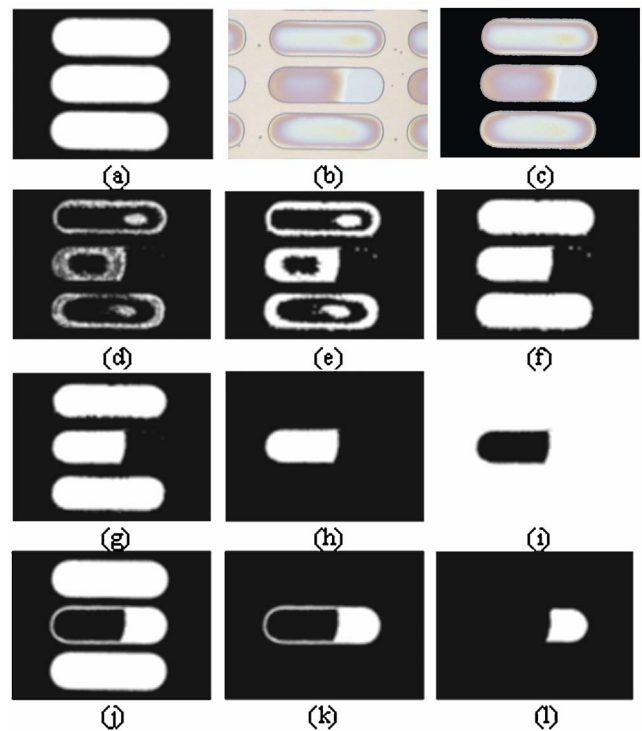


Figure 2. (a)–(l) Unfilled area analysis. (a) Template image before ink jet printing of PEDOT. (b) Original image after ink jet printing of PEDOT. (c) Operation AND between template and original image. (d) Threshold and color abstraction. (e) Dilation. (f) Hole filling operation. (g) Particle filtering for low level pixels. (h) Particle filtering for high level pixels. (i) Invert binary image. (j) Operation AND between template and Fig. 2(i). (k) Band-pass filtering. (l) Erode image by a 7×7 mask.

(10) eliminate noise with filter, as shown in Fig. 1(i);

(11) use Particle analysis to get the data of the satellite drops, as shown in Fig. 1(j).

Defect Type B: Nonuniform Deposition Within the Pixel

The steps of image processing are:

- (1) Get the ellipse area mask from the file, as shown in Fig. 2(a);
- (2) place the mask into first image buffer;
- (3) transform the mask into gray-scale image by extract color plane: HSL-Luminance;
- (4) place the result of (3) into a second image buffer;
- (5) get the image of the PLED substrate from the file, as shown in Fig. 2(b);
- (6) process the mask of first image buffer and the image of PLED substrate by operator AND, as shown in Fig. 2(c);
- (7) convert the image into binary with a pre-determined threshold, leaving pixels in the intervals: Red=[197,223], Green=[164,254], Blue=[140,208];
- (8) filtering the image by smooth-median filter, filtering size=3, to reduce some noise in the image, as shown in Fig. 2(d);
- (9) dilate the image by a 5×5 square structure element in order to enclose certain color area, as shown in Fig. 2(e);

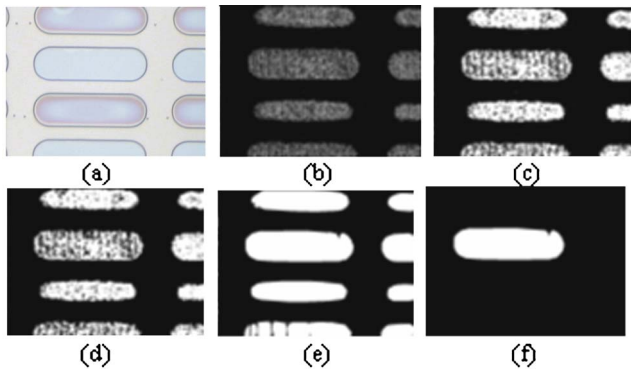


Figure 3. (a)–(f) Omission defects identification. (a) Original image after ink jet printing of PEDOT. (b) Threshold image. (c) Close operation. (d) Smooth-median filtering. (e) Hole filling operation. (f) Band-pass filtering.

- (10) fill up holes in the closed area, as shown in Fig. 2(f);
- (11) erode the image by a 5×5 square structure element in order to fix the magnified area of the previous dilation step;
- (12) use the particle filter function to remove the low-level pixels with values between 0 and 15, as shown in Fig. 2(g);
- (13) use the particle filter function to remove the area of ellipse main axis with values between 400 and 420, as shown in Fig. 2(h);
- (14) invert the binary image, as shown in Fig. 2(i);
- (15) process the image and the mask of the second buffer by operator AND, as shown in Fig. 2(j);
- (16) use band pass filtering to remove certain areas of pixels, as shown in Fig. 2(k);
- (17) erode the image twice by a 7×7 square element in order to eliminate the additional edge and get the unfilled area, as shown in Fig. 2(l);
- (18) calculate data of the unfilled area.

Defect Type C: Pixel Omission

The processing steps are:

- (1) Get the image of the PLED substrate from the file, as shown in Fig. 3(a);
- (2) convert the image into a binary image by a predetermined threshold, leaving pixels within the intervals: Red=[0,216], Green=[0,237], Blue=[238,255], as shown in Fig. 3(b);
- (3) use the “close” technique with a 3×3 square structure element to reduce the holes inside the ellipse, as shown in Fig. 3(c);
- (4) filter the image by smooth-median filter to eliminate isolated particles, filter size=3, as shown in Fig. 3(d);
- (5) use 8-connectivity convex technique forming convex areas to fill the holes inside the ellipse and to smooth the contour of the ellipse, as shown in Fig. 3(e);

- (6) use band pass filter to acquire the area having pixel values between 29,000 and 33,000, i.e., the omission area, as shown in Fig. 3(f);
- (7) get the data of the omission area by particle analysis.

Defect Type D: Interface Between PF and PEDOT Layer

The PF deposited on PEDOT layers will level defects mainly caused by surface treatment and environment deterioration. For PF and PEDOT, both are transparent thin film layer, the challenge is how to increase the discrimination rate. The key solution is to abstract the HSL luminance as process image, instead of the color abstraction. Then following similar processes, the defect can be distinguished and summarized in Table I.

STATISTICS OF DEFECT IDENTIFICATION

To verify the accuracy of this algorithm, we compared the number of defects in the PLED panel by manual operation (optical magnifier) against this auto identification algorithm. Testing panels are labeled from P1–P12. Three types of defects were sought, which were the satellite drop occurrence, unfilled pixel, and pixel omission, as listed in Table II, where the M means the manual observation and AI means the auto identification by this algorithm. If the panel is perfect, it is referred as N/A.

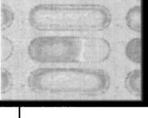
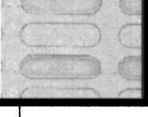
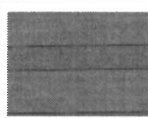
The comparison result of defect identification by manual operation against auto identification algorithm is listed in Table II. The value in the brackets means the difference of identification by manual operation and auto identification algorithm, and the total defects were counted at the end row of table. From Table II, it can be known that the result of AI has good accuracy in defects of unfilled pixel and pixel omission types. It can pick up the errors of manual identification, but it misses some defects of satellite drop occurrence due to the sensitivity of threshold level setting. Overall, the confidence level is larger than 95%.

PATCHING ROUTING AND REFILLING OSCILLATION

The defect analysis is to compare the images against a standard template and to identify the defects of ink jet printing process. When a defect is identified, the position coordinate and the type of defect are recorded for patching purpose afterward. The design processes the defect positions into an optimal patching path so that the ink jet head travels along a shortest path to finish the printing and patching. Figure 4 illustrates the optimal patch path. When applying in patching defects on polymer light emitting diodes, the highly evaporative and viscous ink is easy to dry in the nozzle during a longer idling time of nonprinting. Because the solvent of the ink around the nozzle evaporates, the ink gets a higher viscosity and clogs the nozzle. Therefore, this design provides the optimal patching path for shortening the idling time of the ink jet head during traveling.

Moreover, the invention provides a pre-oscillating driving waveform to the ink jet head for keeping the ink from drying in the nozzle and stabilizing the ink jet printing behavior. The oscillation provides energy to the ink in the

Table I. Summary of versatile image identification scheme used for defect recognition.

Defects	Image processing	Result
 Satellite drop (PF)	Problem: Satellite drop occurred during ink-jet printing Solution : Described above	
 Hole in Pixel (PF)	Problem: Ink drop deposited non-uniform film in pixel or the bank surface is not well treated. Solution : Described above	
 Pixel Omission (PF)	Problem: Pixel omission, some print head nozzles were clogged Solution : Described above	
 Partially Filled Pixel I PEDOT and PF	Problem: Malformed bank or poor ITO layer surface treatment Solution: 1.Acquire image 2.Extract color: HSL-Luminance plane 3.Thresholding: manual 4.Morphology: Erode (5x5) 5.Morphology: Remove small particle 6.Morphology:Fill Holes	
 (PEDOT and PF)Partially unfilled pixel II	Problem: Environment moisture deteriorated device Solution: 1.Acquire image 2.Extract color: HSL-Luminance plane 3.Thresholding: manual 4.Morphology: Remove small particle 5.Morphology:Fill Holes 6.Particle filtering: filter criteria "pixels" 7.Morphology: Dilating (5x5)	

nozzle, but it is less than the amount needed for ejection, so as to prevent the ink from drying and blocking the nozzle. During traveling of the ink jet print head from one patching position to the next, there are pre-oscillating voltage pulses applied on the nozzles of the ink jet print head. When the nozzle reaches the patching position, the nozzle receives a

Table II. Statistics and analysis result of PLED panel by manual identification and auto identification algorithm.

Panel	Defect Description					
	Satellite drop occurrence		Unfilled pixel		Omission	
	M	AI	M	AI	M	AI
P01	7	7	N/A	N/A	1	1
P02	N/A	N/A	N/A	N/A	N/A	N/A
P03	9	9	1	1	N/A	N/A
P04	5	3(-2)	1	2(+1)	N/A	N/A
P05	5	3(-2)	N/A	N/A	N/A	N/A
P06	8	8	1	1	N/A	N/A
P07	4	4	1	1	N/A	N/A
P08	3	3	1	1	N/A	N/A
P09	6	6	2	2	N/A	N/A
P10	7	8(+1)	1	4(+3)	N/A	N/A
P 11	9	9	N/A	N/A	1	1
P 12	7	7	N/A	N/A	1	1
Total	70	67	8	12	3	3
Accuracy	95%		100%		100%	

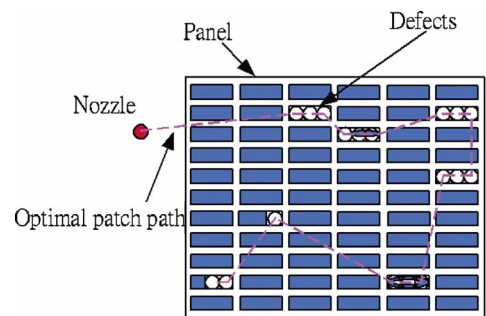


Figure 4. Illustrate optimal patch routine design after defect recognition.

firing voltage and ejects an ink droplet to the defect position. After patching, the pre-oscillation pulses are maintained to prevent the nozzles from clogging.

MULTI-RING ACCUMULATION

In this study, we also observed another interesting problem, multi-rings in the printed pattern. Many studies have been performed on the evaporation of a drop of ink on a substrate,^{15,16} and discuss the behavior of particles accumulating at the contact line and form ordered arrays. Some groups have focused on how particles are distributed after

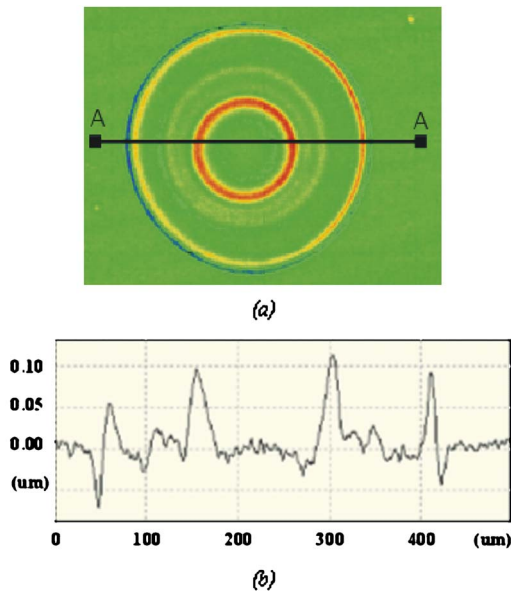


Figure 5. (a) and (b) Multi-ring behavior observed for continuous ink jet printing accumulating up to 10 drops.

the drying process.^{17,18} Adachi et al.¹⁷ observed that circular stripe patterns, i.e., rings, form inside the dried drops, and further noticed that the three phase (water, air, glass) contact line exhibited stick-slip motion as the water evaporated. It is important to note that motion of the contact line really refers to the disappearance of water due to evaporation and not to the lateral physical movement of the particles at the contact line. Shmuylovich¹⁹ studied more detailed features of multi-ring behavior for latex. They concluded that because the evaporation rate in a pinned drop is greatest at the edge, there is a flow of water toward the edge. They reported the results of experiments on concentric ring formation and contact line pinning, and discussed how particle size may affect the way in which the contact line gets pinned. An observation of the particles accumulating at the initial contact line is presented as the evaporation occurred, the contact line moved and multiple rings formed. It is interesting that small drop volume made a small ring area on the substrate, and there was only one ring inside the drop. As the volume increases, the radius of the drop also increases, and bigger multi-rings form.

Figures 5(a) and 5(b) were an observation of continuous ink jet printing of PF ink accumulating up to ten drops above PEDOT layer of glass substrate. A 0.7 mm glass substrate with 1500–2000 Å thickness of ITO is patterned as stripes to define the anode lines. The PEDOT buffer layer thickness was then patterned on top of ITO with thickness around 1000–2000 Å. The whole process is fabricated in a low moisture and low oxygen content dry box. The drop-to-drop firing frequency of PF ink was controlled at 1 Hz. Figure 5(a) was a top view of drop face to substrate, and it indicated the accumulated drop having the diameter size of about 350 μm. Figure 5(b) was the profile along with the

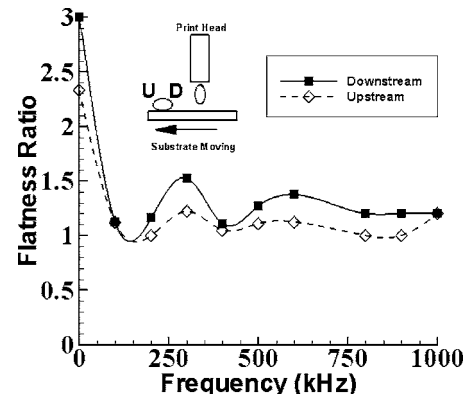


Figure 6. Different operation effects in film morphology of ink jet drops of PF ink. Flatness ratio for downstream and upstream of ink drop at the operation range of 0–1000 kHz.

A-A section in Fig. 5(a). Multi-ring behavior was found in the image, and the peak value was about 0.1 μm. The multi-ring behavior dominates flatness of the film in ink jet patching process, and it must be assisted with complementary method to solve the problem. Recently, a vibration-induced method is proposed by Kevin et al.²³ that found the vibration-induced method substantially changed the polymer film ring edge behavior by shrinking the polymer drop size, and controlling the film uniformity. It changed the flatness ratio (defined as profile peak / profile average) from 3.0 (with coffee ring) to about 1.0 (nearly a flat film), respectively. Figure 6 compared the flatness ratio for downstream and upstream of PF drops at different operation frequency. Upstream (Noted as U) is defined as the drop boundary facing the print head as it moves across the substrate, and the downstream (Noted as D) means the boundary opposite to the upstream. It was clearly found that the downstream side has thicker ring than that of upstream, and presented a higher flatness ratio at various operation frequencies. Takeo²⁰ mentioned the airflow will affect the morphology of drop as drying. Fast convection is helpful to get smoother film. It explained why the ring at upstream is always flatter than that of downstream, and higher frequency will create more stationary wave node in drop surface.

DISCUSSION AND CONCLUSIONS

In this study, we developed an image identification process for recognizing the pixel defect of PEDOT and PF. Due to the thin and highly transparent characteristics of PEDOT and PF layering on low contrast substrate (glass), it was generally hard to find defects. This study successfully observed and recognized these defects, designed a methodology for determining the optimal ink jet printing route, and its driving waveform with refilling oscillations to keep the ink jet print head moist while moving across the substrate. However, the multi-ring behavior occurred during patching by ink jet may be a challenge in this development. The study verified that a physical enforcement was helpful to resolve this problem. Further focus study is expected in near future.

REFERENCES

- ¹C. W. Tang and S. A. Vanslyke, *Appl. Phys. Lett.* **51**, 913 (1987).
- ²J. H. Burroughes, D. D. C. Bradley, A. R. Brown, R. N. Marks, K. Mackay, R. H. Friend, P. L. Burn, and A. B. Holmes, *Nature (London)* **347**, 539 (1990).
- ³R. F. Service, "Organic light emitters gain longevity", *Science* **273**, 878–880 (1996).
- ⁴J. R. Sheats, H. Antoniadis, M. Hueschen, W. Leonard, J. Miller, R. Moon, D. Roitman, and A. Stocking, "Organic electroluminescent devices", *Science* **273**, 884 (1996).
- ⁵A. Shen, P. E. Burrows, and M. E. Thompson, *Science* **276**, 2009 (1997).
- ⁶K. Suzuki, K. Tsukada, Y. Koike, T. Seino, Y. Ouki, Y. Kosugi, T. Saruta, and H. Tsukada, U.S. Patent No. 6431674 (2002).
- ⁷T. Kitahara, U.S. Patent No. 6357846 (2002).
- ⁸S. Ito, K. Okumura, and K. Sho, U.S. Patent No. 6162745 (2000).
- ⁹D. Braun, "Crosstalk in passive matrix polymer LED displays", *Synth. Met.* **92**, 107–113 (1998).
- ¹⁰T. Hebner, C. Wu, D. Marcy, M. Lu, and J. Strum, *Appl. Phys. Lett.* **72**, 519 (1998).
- ¹¹K. Yoshimori et al., *Proc. Asia Display* **98**, 213 (1998).
- ¹²C.-J. Lin, L.-J. Chen, H.-M. Tsai, F.-K. Chen, Y.-Z. Lee, J. P. Lu, K.-T. Lin, and K. Cheng, "Method of patching element defects by ink jet printing", *Proc. IS&T's NIP20* (IS&T, Springfield, VA, 2004) pp. 250–255.
- ¹³M. Morra, E. Occhiello, and F. Garbassi, *Prog. Surf. Sci.* **79**, 13 (2005).
- ¹⁴C.-F. Sung, F.-K. Cheng, H.-M. Tsai, J.-P. Lu, J.-P. Hu, Y.-Z. Lee, J. Chang, and K. Cheng, *Proc. IS&T's NIP20* (IS&T, Springfield, VA, 2004) p. 867.
- ¹⁵N. D. Denkov, O. D. Velez, P. A. Kralchevsky, I. B. Ivanov, H. Yoshimura, and K. Nagayama, *Nature (London)* **361**, 7 (1993).
- ¹⁶C. D. Duskin, H. Yoshimura, and K. Nagayama, *Chem. Rev. Lett.* **204**, 5 (1993).
- ¹⁷E. Adachi, A. S. Dimitriov, and K. Nagayama, *Langmuir* **11**, 1057 (1995).
- ¹⁸R. D. Deegan, O. Bakajin, T. F. Dupont, G. Huber, S. R. Nagel, and T. A. Witten, "Contact line deposits in an evaporating drop", *Phys. Rev. E* **62**, 1 (2000).
- ¹⁹L. Shmuylovich, A. Q. Shen, and H. A. Stone, "Surface morphology of drying latex films: Multiple ring formation", *Langmuir* **18**(9), 3441 (2002).
- ²⁰T. Kawase, "Deposition of soluble materials", International Patent WO 01/70506 (2002).
- ²¹P. May, *SID'96 Digest*, 192 (1996).
- ²²K. Morii and T. Shimoda, "Film formation by ink jet behavior of ink jet droplets", *Japan Surf. Sci.* **24**(2), 90 (2003).
- ²³K. Cheng, W. W. W. Chiu, L.-J. Chen, C. F. Lu, J. Chang, and T.-F. Ying, "Thin film morphology controlled by vibration induced method during ink jet printing", *Appl. Surf. Sci.* (to be published).